

MT25

25th International Conference
on Magnet Technology

RAI - Amsterdam
August 27 - September 1, 2017



Study on Counter-rotating Dual Rotors Radial Permanent magnet Motor for Underwater Vehicle Propulsion

Guangwei Liu, Guohua Qiu, Jinhua Chen,
JinShi, Fengge Zhang

Shenyang University of Technology

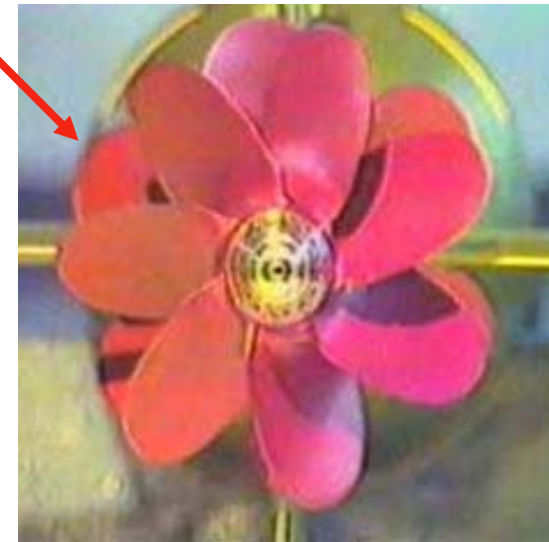
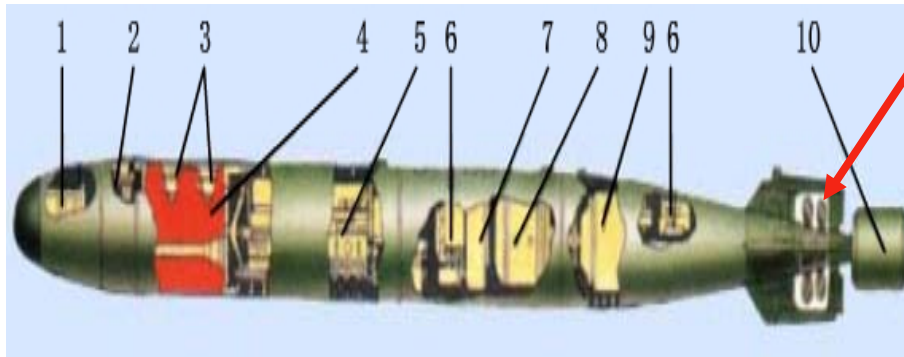
CONTENTS

- 1** Introduction
- 2** Principles and Features
- 3** Design Guidelines
- 4** Finite-element Analysis
- 5** Prototype and Experimental
- 6** Conclusions



Introduction

counter-rotation propeller

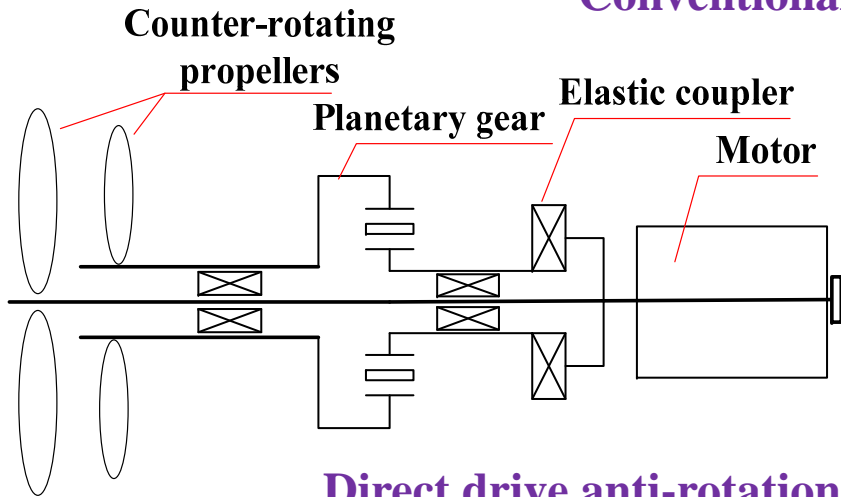


Benefits

- ✓ avoid lateral rotation phenomenon
- ✓ Improved operational efficiency of the system

Introduction

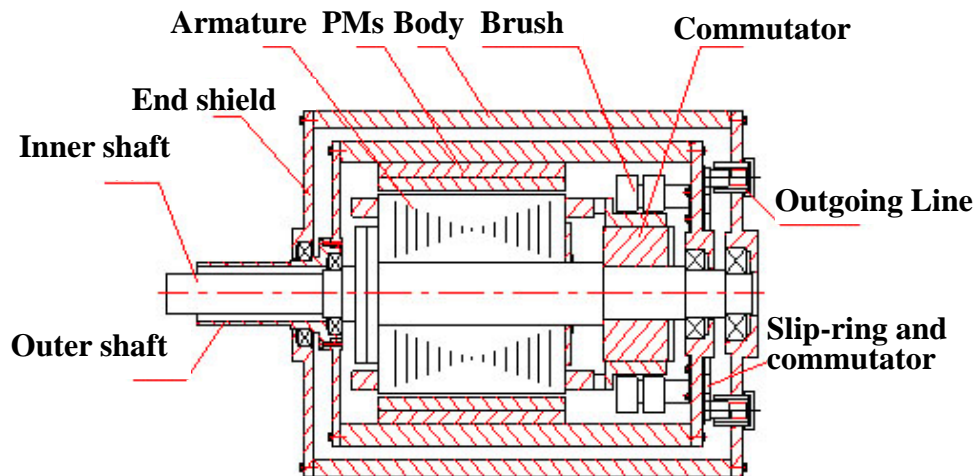
Conventional motor drive



1. Conventional motor and planetary gears

- Large volume
- Complicated structure
- Heavy weight
- Low efficiency
- Low reliability

Direct drive anti-rotation propeller propulsion system



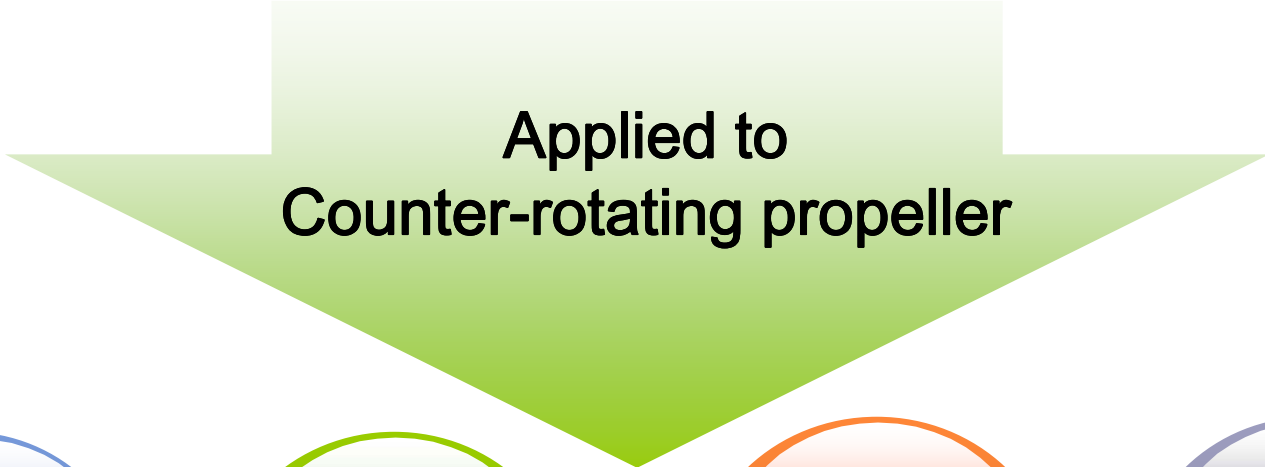
2. PMDC motor with two rotors

Two sets of slip-ring and commutator

Low reliability

Introduction

PM Machine with Counter-rotating Dual Rotors (PMCDR)



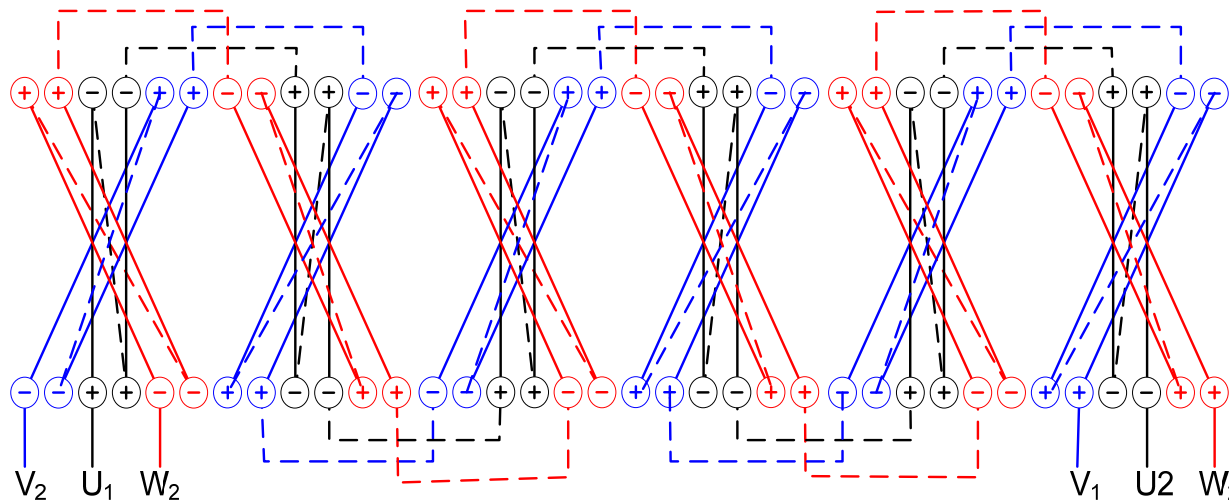
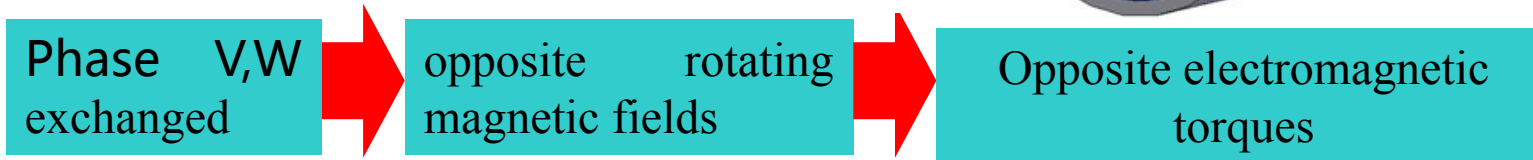
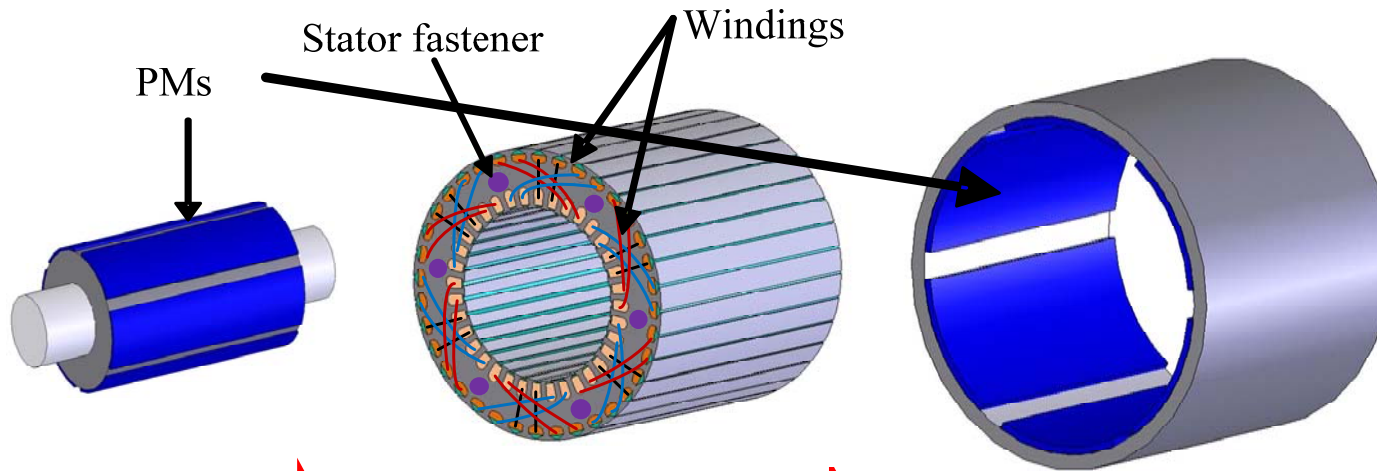
High
Reliability

High
Efficiency

Light
Weight

High
Power density

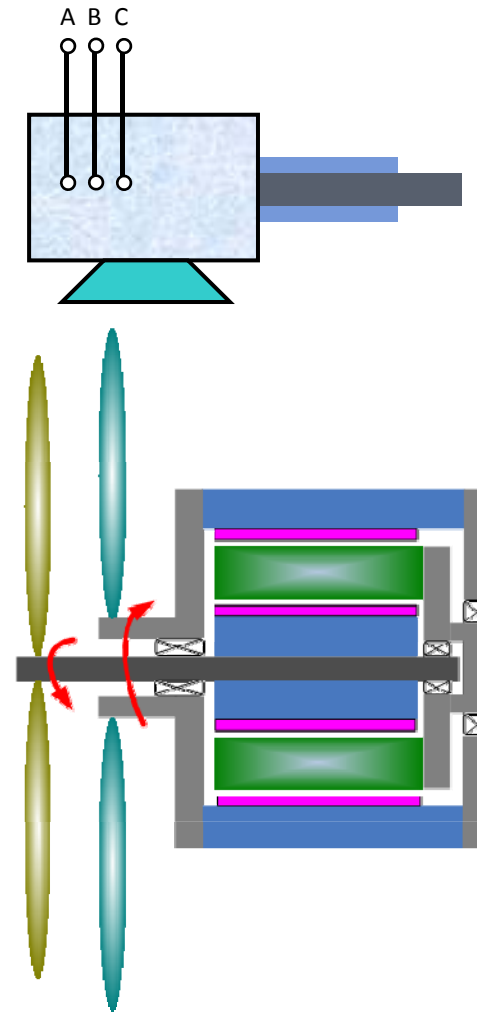
Principles



end connections mode

Features

- single electric power input and dual mechanical torque output
- Rotor-stator-rotor structure
- Back-to-back toroidal winding
- without brush and slip-ring



Advantages and disadvantage

Advantages

- Very short end winding;
- Increase reliability without brush and slip-ring;
- Radial forces balanced and tangential forces can be reduced zero on the stator;
- Little armature reaction;

Disadvantage

- it is not suitable for fractional horsepower machines, since the cross section is too small to hold the rotor-stator-rotor structure.

Machine Design Equations

$$\begin{array}{ccccccc} \text{Same speed} & & \text{Same current} & & \text{Same turns} & & \text{Same core length} \\ \frac{T_{emi}}{T_{emo}} & \propto & \frac{P_{emi}}{P_{emo}} & \propto & \frac{E_i}{E_o} & \propto & \frac{\Phi_i}{\Phi_o} & \propto & \frac{R_i B_{\delta i}}{R_o B_{\delta o}} \end{array}$$

Because UV counter-rotation propeller propulsion system needs the PMCDR to provide two opposite-direction same torques, **the ratio of air-gap flux densities is inverse proportion with radius of two air gaps.**

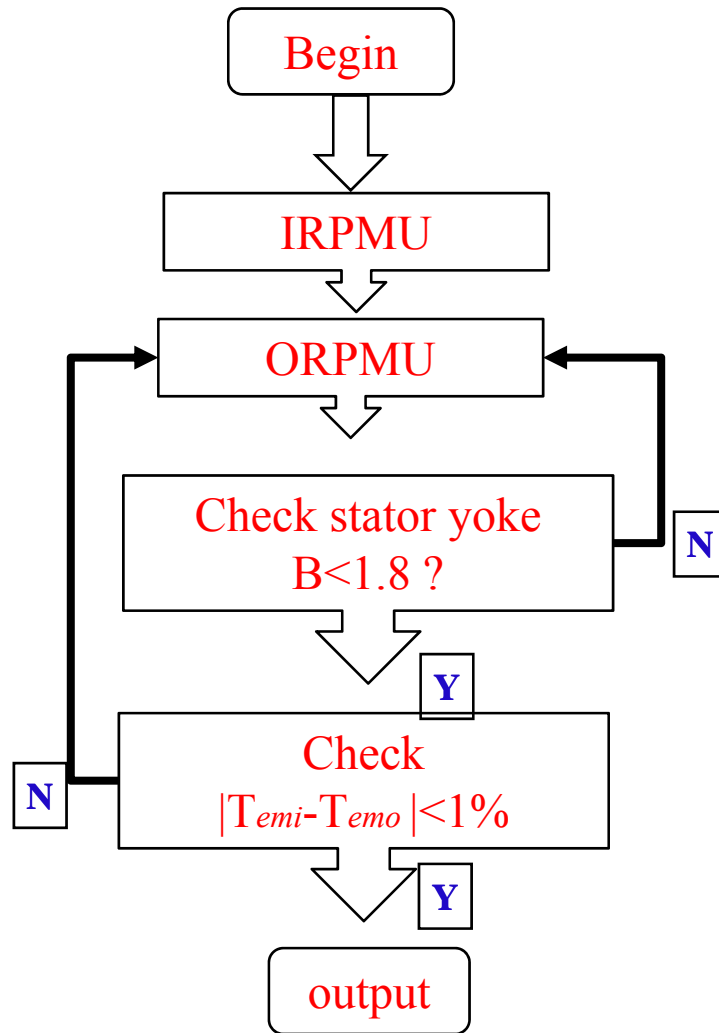
$$B_i / B_o = R_o / R_i$$

Power angle characteristic should be uniform or similar, For UV counter rotation propeller propulsion system, so **the armature reaction reactance should be equal or approximate** for IRPMU and ORPMU.

$$\left. \begin{array}{l} L_{di} = L_{do} \\ L_1 = p q n_s^2 \mu_0 L_{ef} \lambda_1 \\ L_{md} = L_{mq} = \frac{3}{\pi} (q n_s K_{NI})^2 \frac{\mu_0 (D_1 - \delta_i) L_{ef}}{\delta_e + h_m} \end{array} \right\} \left. \begin{array}{l} \frac{(D_{1i} - \delta_i)}{(D_{1o} - \delta_o)} = \frac{\delta_{ei} + h_{mi} / \mu_r}{\delta_{eo} + h_{mo} / \mu_r} = \frac{B_{\delta o}}{B_{\delta i}} \end{array} \right\}$$

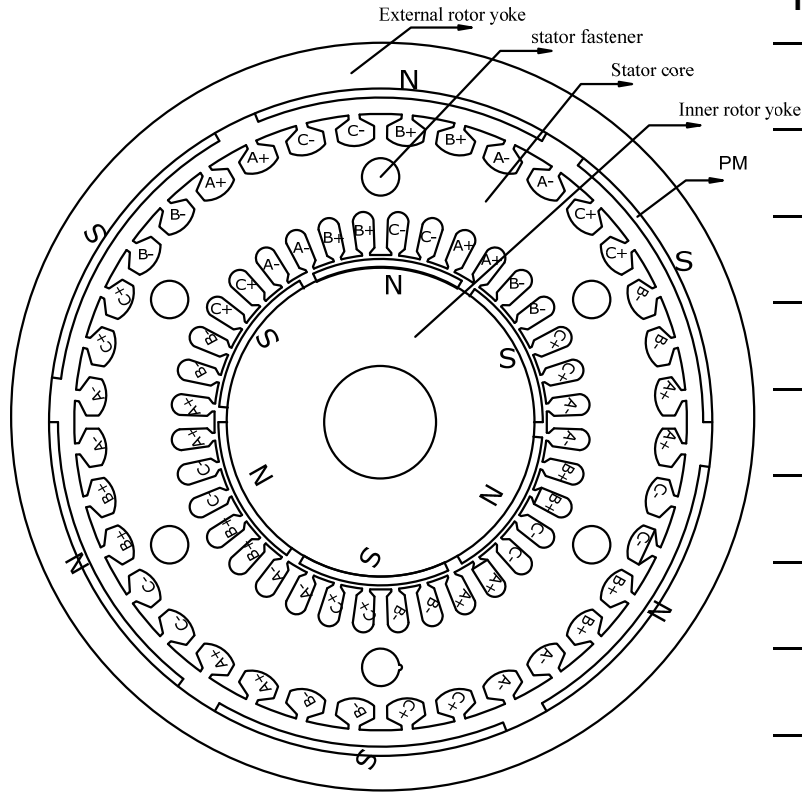
$$h_m = \frac{K_\delta \mu_r}{B_r / B_\delta - 1} \delta \quad \Rightarrow \quad \frac{h_{mo}}{h_{mi}} = \frac{B_{ro}}{B_{ri}} = K$$

Design guidelines



Each portion (IRPMU and ORPMU) design can be similar with the conventional surface-mounted PM design process, but the winding area, coil turns, and current density have to be same for two portions. there will be an iteration in each inner or outer portion design.

Finite Element Analysis



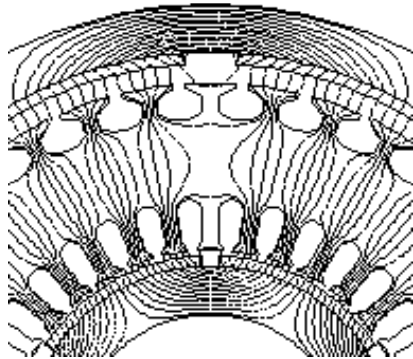
2-D solid model of PMCDR

Main Dimensions and Parameters of PMCDR

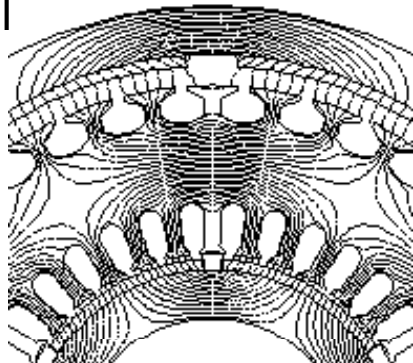
Rated voltage (V)	300
Stator winding connection	Y
Rated frequency (Hz)	40
Inner diameter of stator core (mm)	125
Outer diameter of stator core(mm)	230
Inner diameter of inner rotor(mm)	75
Outer diameter of inner rotor(mm)	115.2
Inner diameter of outer rotor(mm)	249
Outer diameter of outer rotor(mm)	279
Effective length(mm)	198

Finite Element Analysis

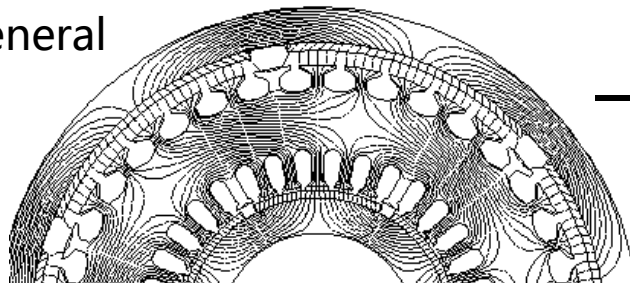
Series



Parallel



General

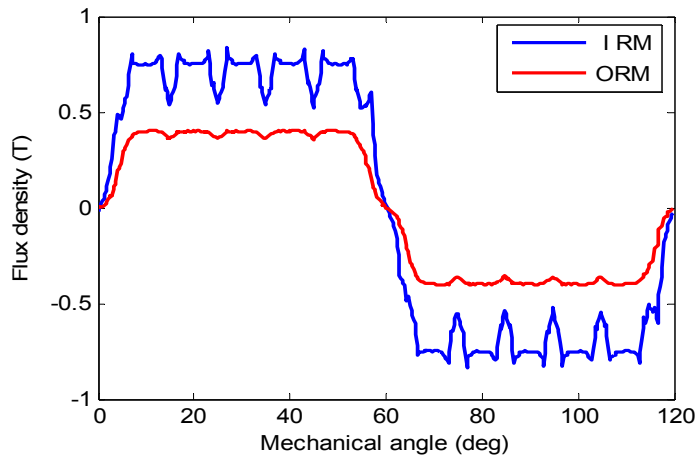


Comparison of the EMC and FEM for PMCDR

	EMC		FEM	
	No load	Rated load	No load	Rated load
B_{yi}/T	0.546	0.571	0.514	0.527
B_{ti}/T	1.556	1.631	1.492	1.623
B_{to}/T	1.525	1.633	1.423	1.615
B_y/T	1.575	1.668	1.213	1.352
B_{yo}/T	1.334	1.429	1.270	1.274
T_{emi}/Nm		70.07		69.29
T_{emo}/Nm		72.86		71.12

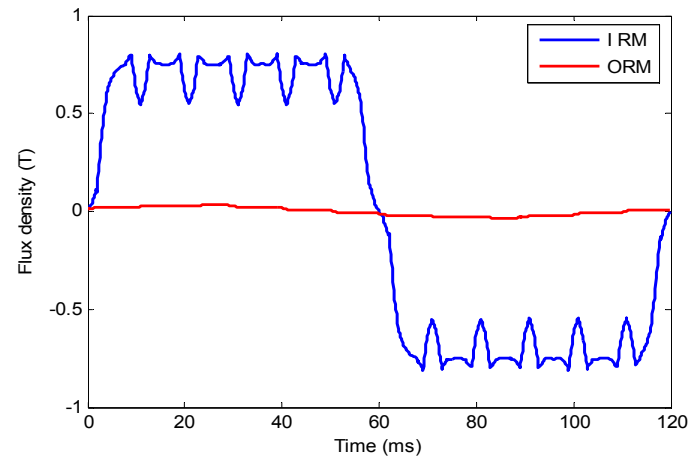
series and parallel magnetic flux path of the machine is periodic change with two rotor positions cyclical change.

Finite Element Analysis

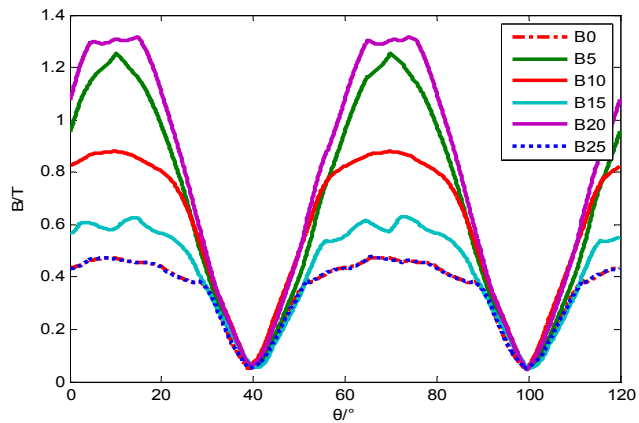


Both inner and outer rotor PM

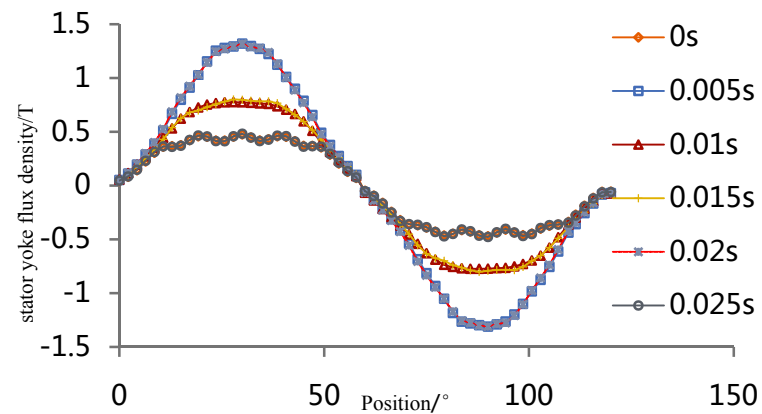
No-load air gap flux density of IRPMU and ORPMU



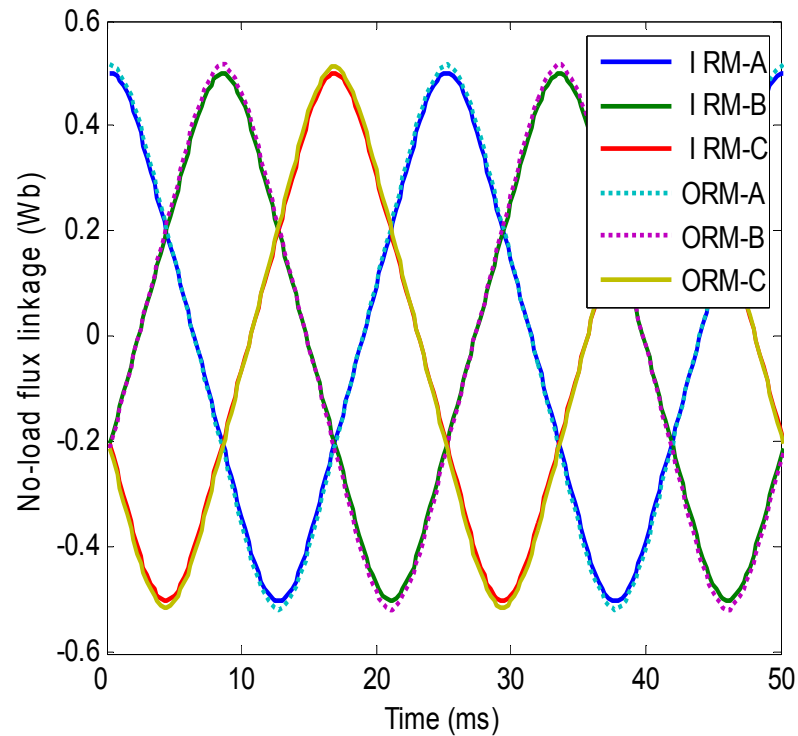
Only Inner rotor PM



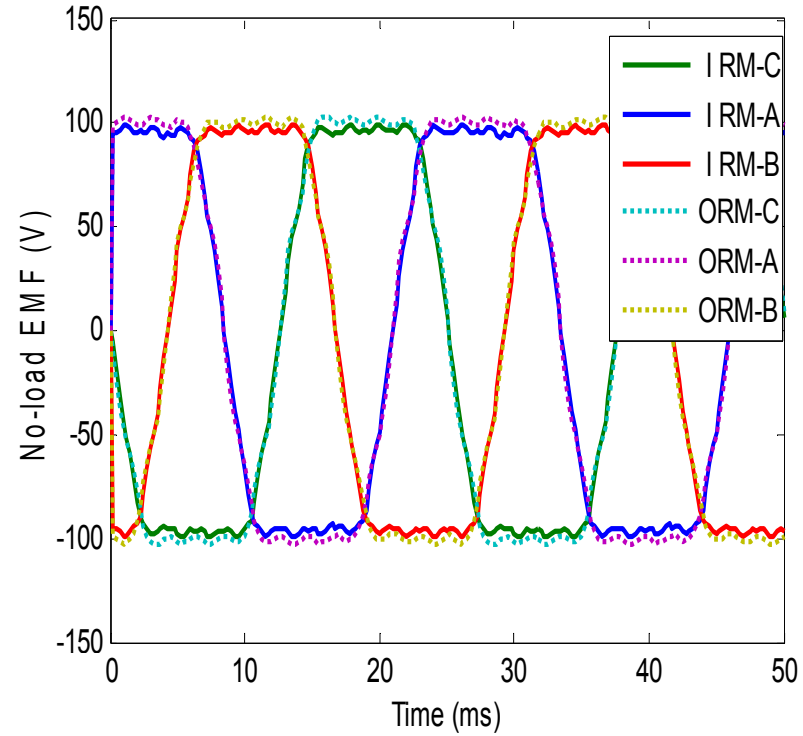
Curves of stator yoke flux density at different times



Finite Element Analysis



No-load air gap flux linkage

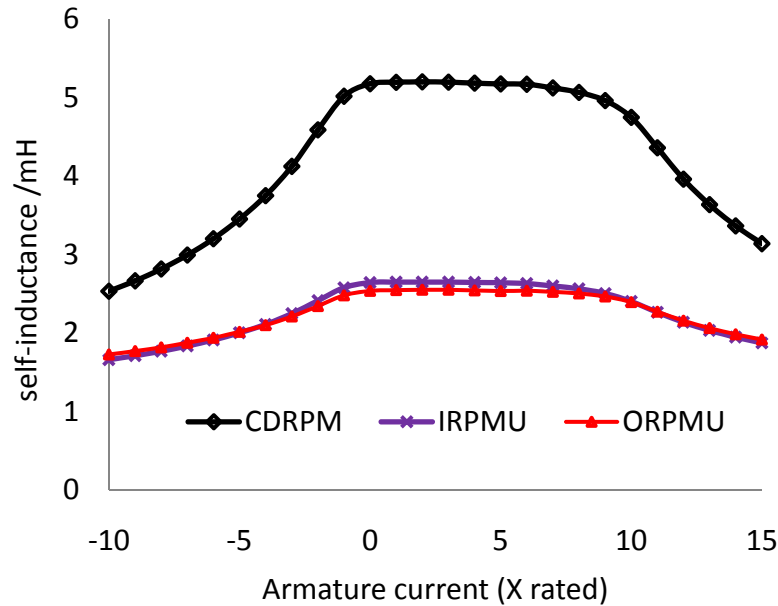


Phase-to-neutral back EMFs waveforms

the air gap flux linkage/ back EMFs of the IRPMU and ORPMU are almost the same value, separately

Finite Element Analysis

Inductance



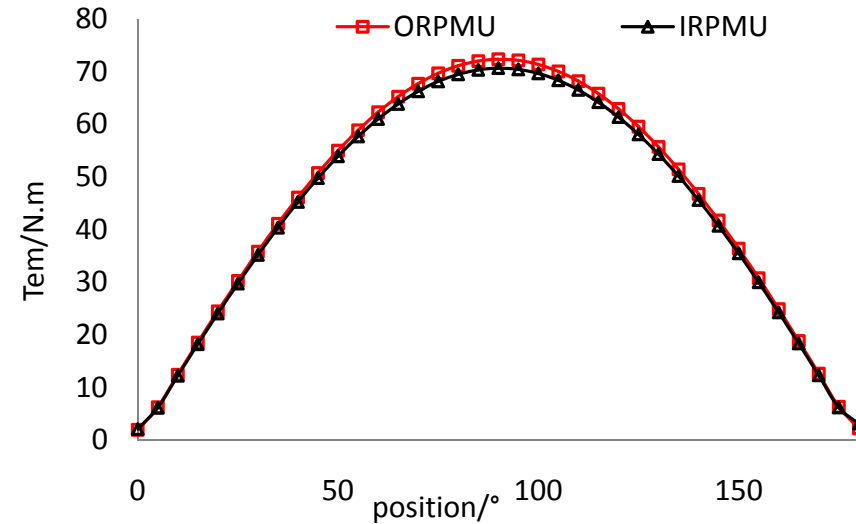
Curve of incremental inductance varying with current

demagnetization current reaches the rated 9 times, forming a reverse magnetic saturation, and when increased 1 times of the rated current, already being saturated.

Torque angle characteristic

$$T_{em} = \frac{mE_1U_1}{X_{d1}\Omega} \sin \theta' = \frac{mE_2U_2}{X_{d2}\Omega} \sin \theta''$$

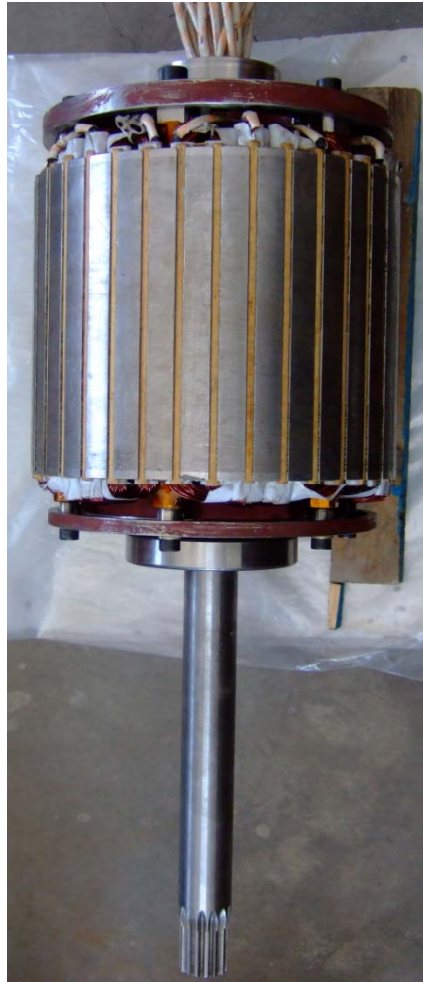
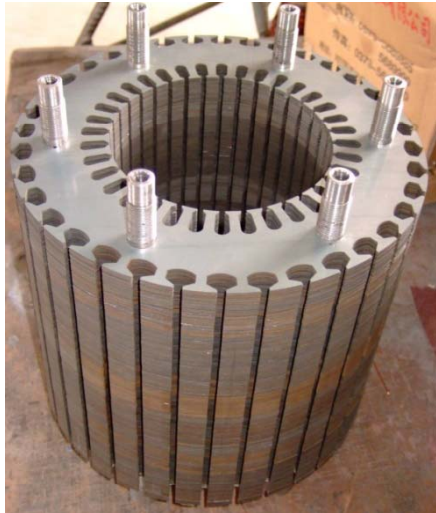
$$= K_1 \sin \theta' = K_2 \sin \theta'' = K \sin \theta$$



Curves of torque angle of PMCDR

torque angle characteristic between IRPMU and ORPMU corresponding to the same.

Prototype and Experimental



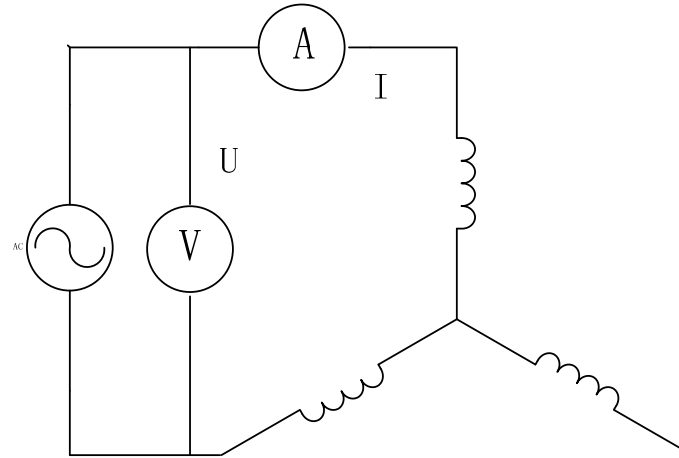
Prototype machine

Prototype and Experimental

Inductance measurements

$$L_d = \frac{1}{4\pi f} \sqrt{\left(\frac{U}{I_{\min}}\right)^2 - R^2}$$

$$L_q = \frac{1}{4\pi f} \sqrt{\left(\frac{U}{I_{\max}}\right)^2 - R^2}$$



Inductance measurement setup for the volt-ampere method

Data of inductance with PMCDR

	Calculated				Measured	
	EMC		FEA		L_d /mH	L_q /mH
	L_d /mH	L_q /mH	L_d /mH	L_q /mH		
IRPMU	3.31	3.22	3.34	3.28	3.95	3.85
ORPMU	3.27	3.22	3.23	3.20		
CDRPM	6.58	6.44	6.57	6.48	6.32	6.09

Prototype and Experimental

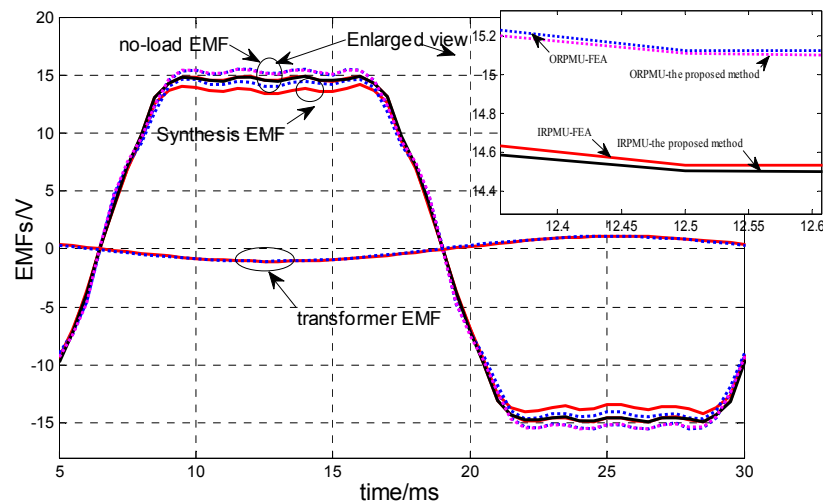
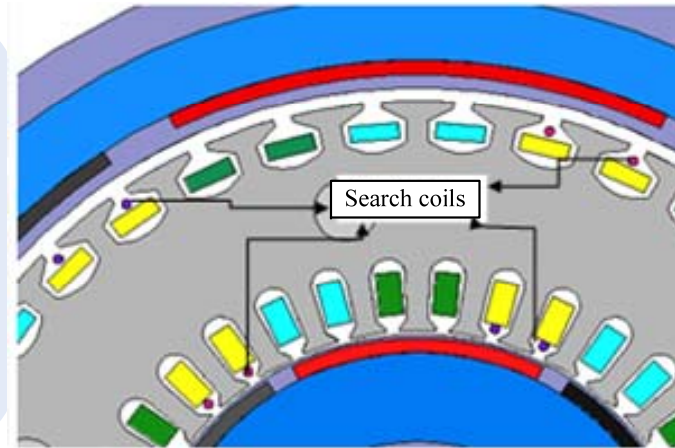
Back-EMFs measurement

$$e = -\frac{d\Psi}{dt} = -\frac{\partial\Psi}{\partial t} - \frac{\partial\Psi}{\partial\theta} \frac{d\theta}{dt} = e_t + e_v$$

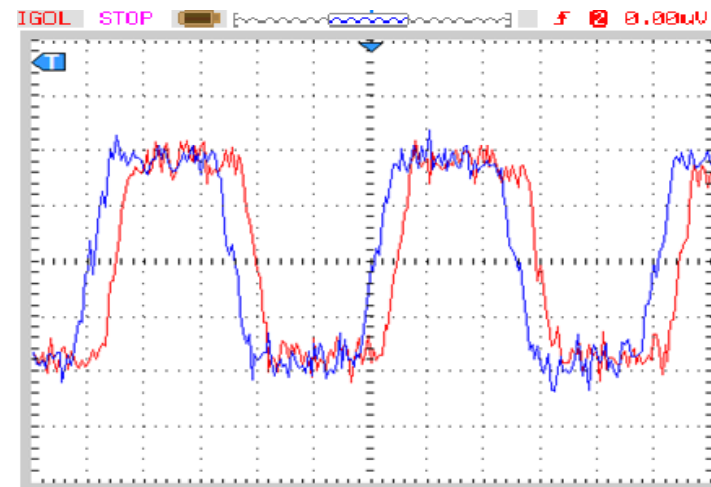
$$e_t = \frac{d\Psi}{dt} = \frac{d(\psi_{pm} + \psi_a)}{dt} = \frac{d(\psi_{pm} + k_a Ni\Lambda)}{dt} = k_{t1} \frac{d(i\Lambda)}{dt} = k_{t1} \Lambda \frac{di}{dt}$$

$$e_0 = e_v \frac{k_{NI} N}{nn}$$

Test principle



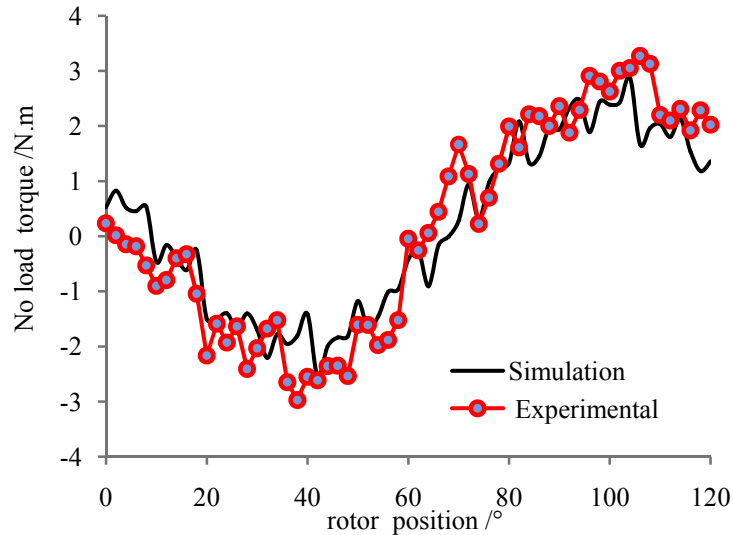
Curves of EMFs versus time with one third of the rated current



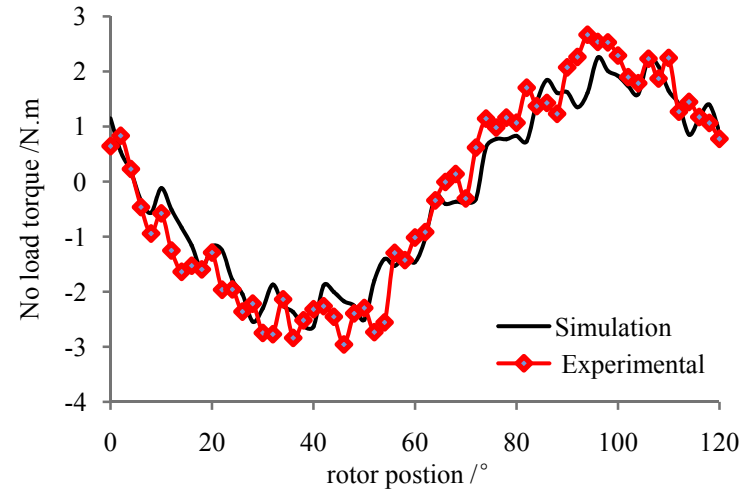
Curves of EMFs versus time with 1/2 rated speed for PMCDR

Prototype and Experimental

No load torque



A) IRPMU



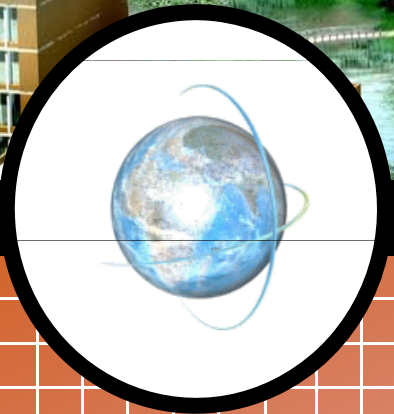
B) ORPMU

No load torque ripples for IRPMU and ORPMU versus rotor position

the effective reduction of cogging torque by means of rotor skewing pole by a stator slot pitch, but the torque periodic due to the inner and outer permanent magnet attraction and repulsion between the rotors is a pole pitch.

CONCLUSIONS

- Magnetic field of the stator yoke is pulsating magnetic field.
- series and parallel magnetic flux path of the machine is periodic change with two rotor positions cyclical change.
- The ratio of air-gap flux densities is inverse proportion with radius of two air gaps, and the magnetization direction of the permanent magnet external rotor length than the inner rotor permanent magnet is slightly larger in order to meet power angle characteristic corresponding to uniform or similar between IRPMU and ORPMU.
- the air gap flux linkage, back EMFs , inductance and Torque angle characteristic of the IRPMU and ORPMU are almost same, separately.
- Search coils are adopted to detecting no-load back-EMFs. The validity is verified by FEA results and experimental measurements



Thanks!



沈陽工業大學
SHENYANG UNIVERSITY OF TECHNOLOGY